

Supplementary Information

Effect of local coordination on catalytic activities and selectivities of Fe-based catalysts for N₂ reduction

Xiaohui Zhang,^a Tianyi Wang,^{b,c} Congyun Zhang,^a Yihui Zou,^a Jun Ren,^d Pengcheng Cai,^a Chenghua Sun,^{*,b,c} and Dongjiang Yang^{*,a,e}

^aSchool of Environmental Science and Engineering, State Key Laboratory of Biofibers and Eco-textiles, Shandong Collaborative Innovation Center of Marine Biobased Fibers and Ecological Textiles, Qingdao University, Qingdao 266071, P. R. China

^bSchool of Chemical Engineering and Energy Technology, Dongguan University of Technology, Dongguan 523808, P. R. China

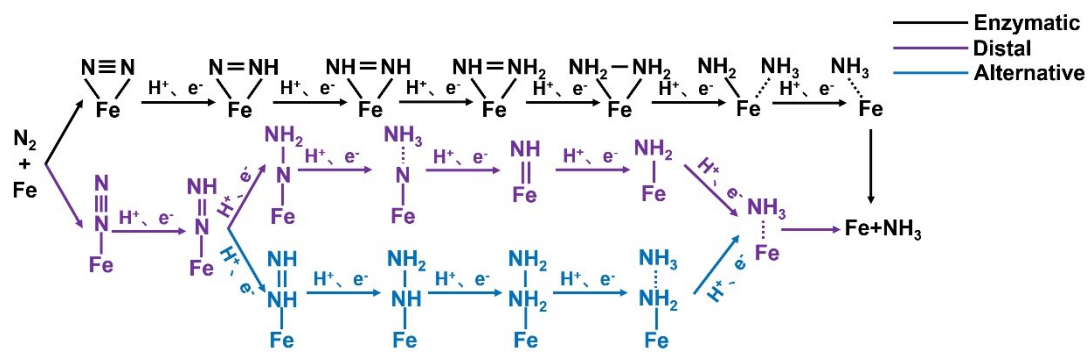
^cDepartment of Chemistry and Biotechnology and Centre for Translational Atomaterials, Faculty of Science, Engineering and Technology, Swinburne University of Technology, Hawthorn, Victoria 3122, Australia

^dSchool of Chemical and Environmental Engineering, North University of China, Taiyuan, 030051, P. R. China

^eQueensland Micro- and Nanotechnology Centre (QMNC), Griffith University, Nathan Campus, Brisbane, Queensland, 4111, Australia

*Corresponding authors: chenghuasun@swin.edu.au (C. Sun);

d.yang@qdu.edu.cn (D. Yang)



Scheme: Schematic depiction of three mechanisms for NRR on $\text{Fe}_{1/2/3}\text{C}_x\text{N}_y$. The Fe represents the Fe atom active on the electrocatalyst.

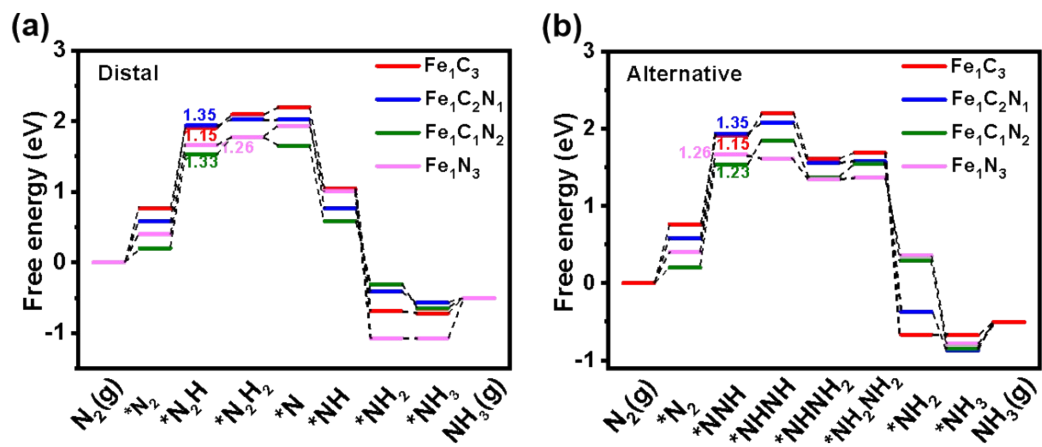


Fig. S1 Free energy diagrams of $\text{Fe}_1\text{C}_x\text{N}_y$ on (a) distal pathway, (b) alternative pathway and (c) enzymatic pathway.

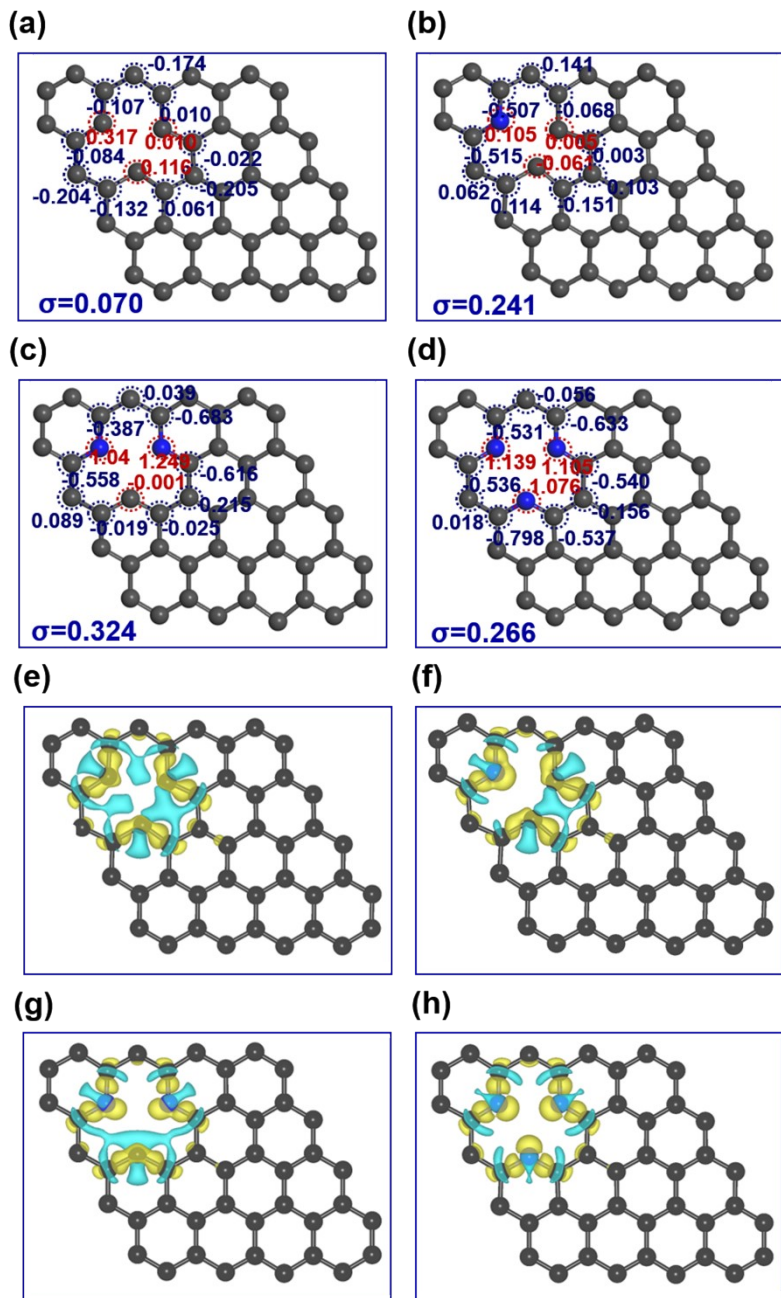


Fig. S2 (a)-(d) The number of Bader charge for the carbon atoms on the different C_xN_y ligand environments; (e)-(h) the charge density difference of the corresponding ligand environment.

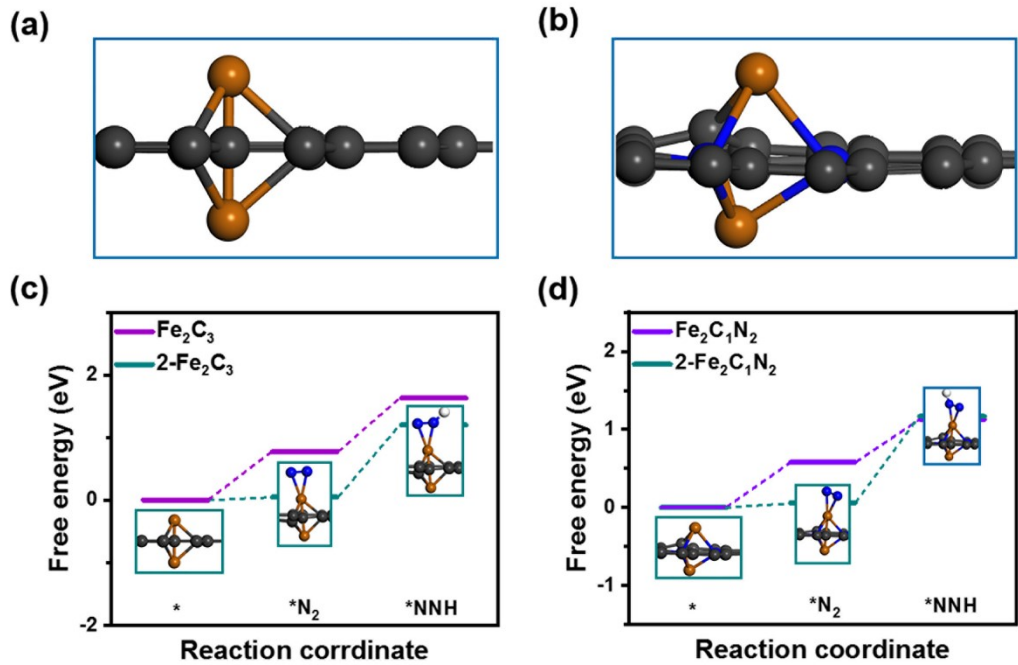


Fig. S3 The side views of geometry structure of (a) 2-Fe₂C₃ and (b) 2-Fe₂C₁N₂; (c) schematic depiction of the reaction pathways of Fe₂C₃ and 2-Fe₂C₃; (d) schematic depiction of the reaction pathways of Fe₂C₁N₂ and 2-Fe₂C₁N₂.

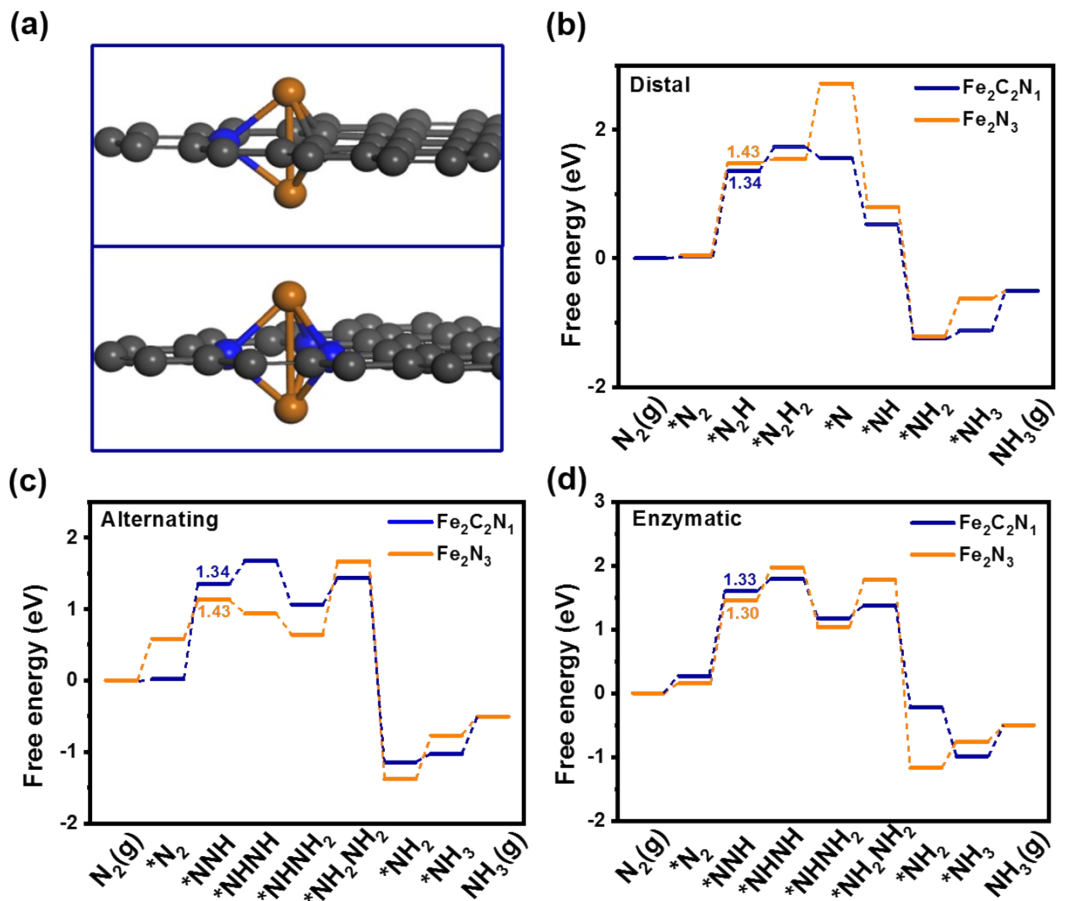


Fig. S4 The side views of geometry structure of (a) $\text{Fe}_2\text{C}_2\text{N}_1$ and Fe_2N_3 ; free energy diagrams of $\text{Fe}_2\text{C}_2\text{N}_1$ and Fe_2N_3 on (b) distal pathway, (c) alternative pathway and (d) enzymatic pathway.

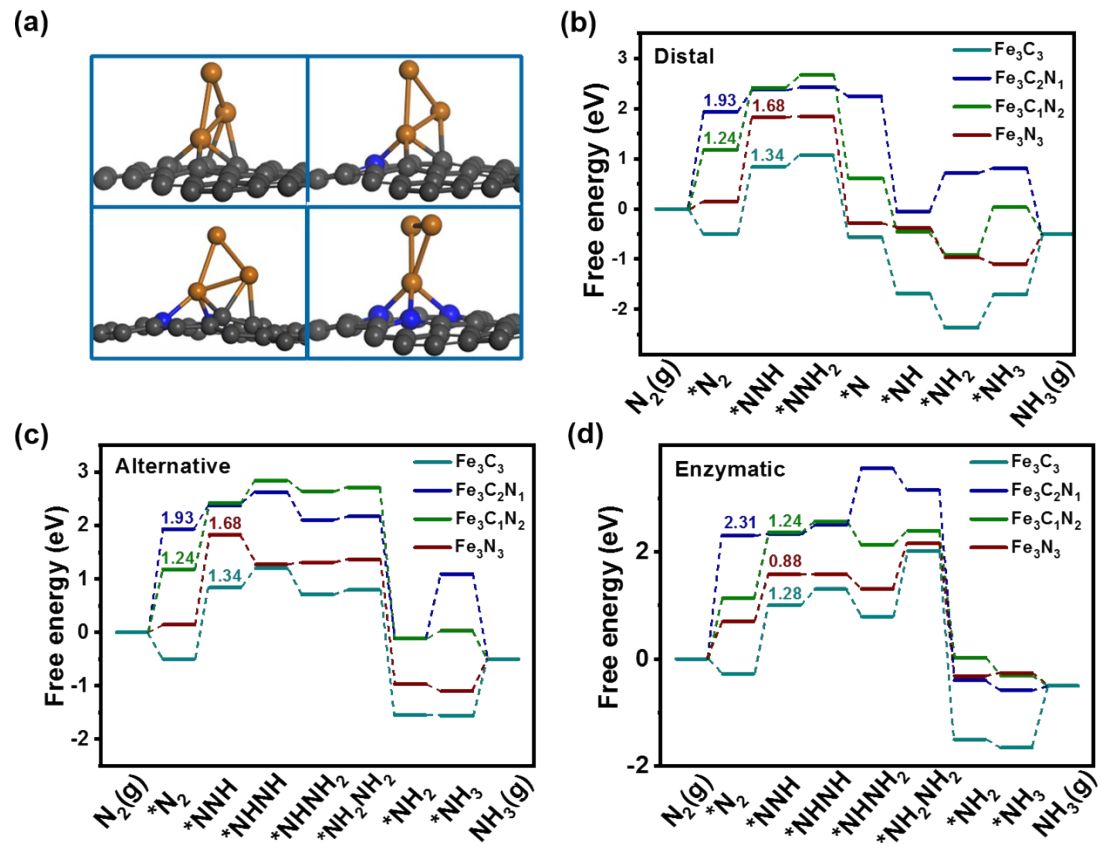


Fig. S5 The side views of geometry structure of (a) Fe_3C_3 , (b) $\text{Fe}_3\text{C}_2\text{N}_1$, (c) $\text{Fe}_3\text{C}_1\text{N}_2$ and (d) Fe_3N_3 ; free energy diagrams of $\text{Fe}_3\text{C}_x\text{N}_y$ on (c) distal pathway, (d) alternative pathway and (e) enzymatic pathway.

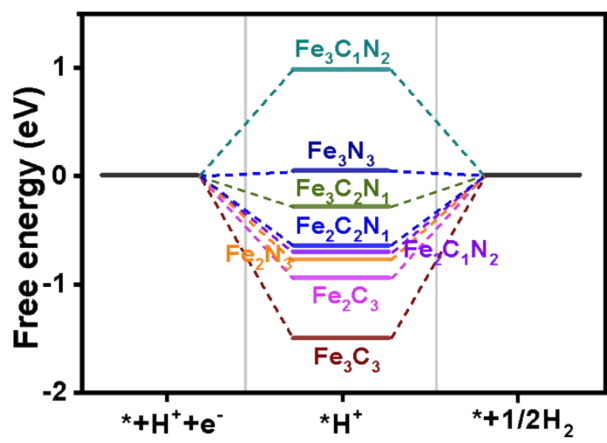


Fig. S6 Free energy diagrams of the HER on the catalysts.

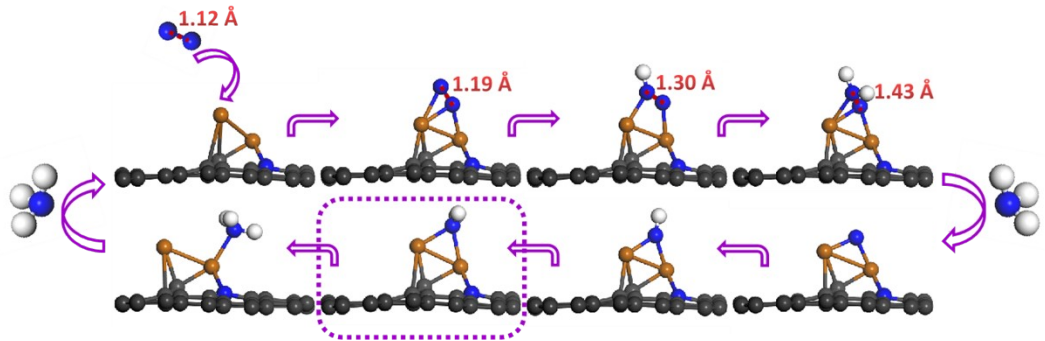


Fig. S7 The corresponding intermediate configurations on the distal pathways of $\text{Fe}_2\text{C}_1\text{N}_2$.

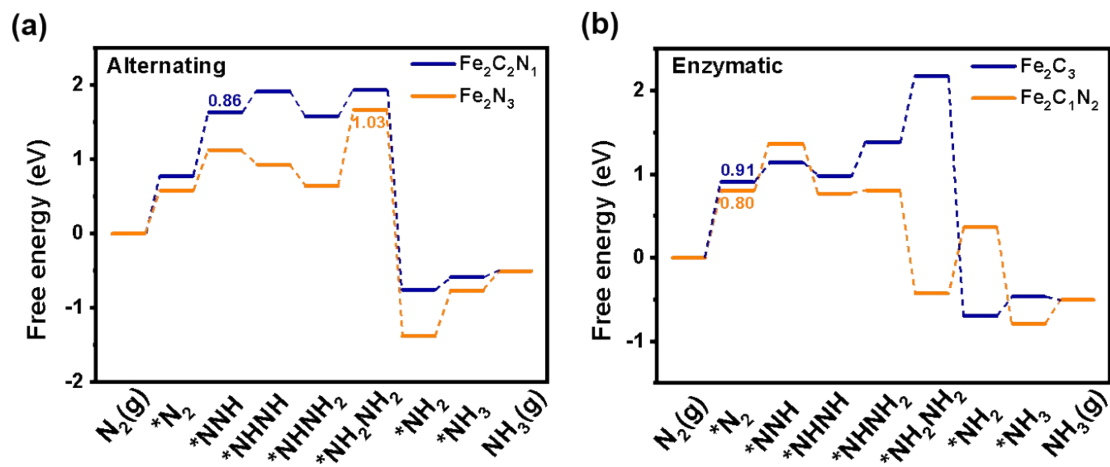


Fig. S8 Free energy diagrams of Fe₂C₃ and Fe₂C₁N₂ on (a) alternative pathway and (b) enzymatic pathway.

Table S1 The calculated ΔZPE and $T\Delta S$ of various NRR reaction intermediates of $\text{Fe}_{1/2/3}\text{C}_x\text{N}_y$.

Adsorption species	ΔZPE (eV)	$T\Delta S$ (eV)
*N ₂	0.156	0.116
*NNH	0.350	0.183
*NNH ₂	0.731	0.179
*N	0.027	0.118
*NH	0.266	0.117
*NH ₂	0.624	0.179
*NH ₃	0.951	0.149
*NHNH	0.827	0.207
*NHNH ₂	1.115	0.243
*NH ₂ NH ₂	1.475	0.160
*NH ₂	0.624	0.179
*NH ₃	0.951	0.149

Table S2 The average of the Bader charge on the different C_xN_y ligand environments.

Ligand Environment	Average (e)
C_3	-0.111
C_2N_1	-0.092
C_1N_2	-0.216
N_3	-0.419

Table S3 N≡N bond length, Bader charge of the absorbed N₂ and calculated ΔG_{max}

for the catalysts.

Catalyst	d _{N-N} (Å)	Charge (e)	ΔG _{max} (eV)
Fe ₂ C ₂ N ₁	1.17	0.38	1.33
Fe ₂ N ₃	1.18	0.34	1.30
Fe ₃ C ₃	1.15	0.24	1.28
Fe ₃ C ₂ N ₁	1.13	0.22	1.93
Fe ₃ C ₁ N ₂	1.15	0.28	1.24
Fe ₃ N ₃	1.16	0.41	0.88

Table S4 The ΔG_{\max} of PLS for NRR on different catalysts.

Catalysts	ΔG_{\max} (eV)	References
Fe(110)	1.39	10.1039/c8cy01845f. ¹
Ti@N ₄	0.69	10.1021/acscatal.8b00905. ²
Fe-Ti _{DA} /GS	0.88	10.1016/j.electacta.2020.135667. ³
MoS ₂	0.68	10.1002/adma.201800191. ⁴
Fe _{SA} /MoS ₂	1.01	10.1039/c7cp08626a. ⁵
Fe@Fe-N ₃ /C-CNTs	1.66	10.1021/acscatal.8b03802. ⁶
FeN ₄ -NG	1.12	10.1016/j.jcat.2020.05.009. ⁷
Fe₂C₁N₂	0.62	This work

Table S5 The atomic fractional coordinates of the Fe₂C₃.

Atom	X	Y	Z
C	0.991819	0.002322	0.082669
C	0.125036	0.068823	0.083569
C	0.191746	0.002273	0.083545
C	0.325073	0.068817	0.084820
C	0.391873	0.002292	0.086427
C	0.525046	0.068754	0.086698
C	0.591545	0.001821	0.088759
C	0.724938	0.068794	0.085191
C	0.791626	0.002292	0.084716
C	0.924968	0.068802	0.082801
C	0.991424	0.202115	0.084009
C	0.124522	0.268378	0.088175
C	0.191513	0.201997	0.087484
C	0.324628	0.267968	0.090967
C	0.391857	0.201971	0.087356
C	0.525192	0.268329	0.087691
C	0.591870	0.201906	0.085529
C	0.725004	0.268632	0.084301
C	0.791625	0.202101	0.083447
C	0.924868	0.268791	0.083940
C	0.991864	0.402341	0.086284
C	0.123889	0.468455	0.093871
C	0.190529	0.401424	0.096403
C	0.320682	0.461627	0.107968
C	0.391102	0.400982	0.099528
C	0.525309	0.467333	0.097553
C	0.592040	0.401630	0.090443
C	0.725297	0.468560	0.086507
C	0.791706	0.401895	0.084095
C	0.924929	0.468830	0.084142
C	0.991551	0.602062	0.083987
C	0.124592	0.668973	0.087958
C	0.190607	0.602262	0.097089
C	0.320208	0.672245	0.110253
C	0.531160	0.672409	0.109078
C	0.592893	0.602476	0.098414
C	0.726379	0.669273	0.090038
C	0.792108	0.602038	0.086097
C	0.925246	0.669016	0.083338
C	0.991885	0.802392	0.082905
C	0.125134	0.869039	0.083344

C	0.191645	0.802324	0.086907
C	0.324843	0.869059	0.089787
C	0.391295	0.802648	0.098993
C	0.525341	0.869675	0.096257
C	0.592370	0.803097	0.097673
C	0.725199	0.869160	0.088928
C	0.792117	0.802529	0.087672
C	0.925301	0.869100	0.083573
Fe	0.391124	0.599318	0.162874
Fe	0.567721	0.572559	0.211729

Table S6 The atomic fractional coordinates of the Fe₂C₁N₂.

Atom	X	Y	Z
C	0.991068	0.004627	0.175106
C	0.124327	0.071368	0.176612
C	0.190949	0.004547	0.175142
C	0.324267	0.071084	0.177853
C	0.390936	0.004295	0.179953
C	0.523879	0.069829	0.182914
C	0.589072	0.000977	0.185267
C	0.723195	0.069815	0.182611
C	0.790853	0.004481	0.179570
C	0.924162	0.071197	0.177799
C	0.990529	0.204342	0.183126
C	0.123337	0.270465	0.188737
C	0.190402	0.204110	0.184038
C	0.323600	0.270063	0.187832
C	0.390797	0.204269	0.182788
C	0.524168	0.271183	0.186079
C	0.590609	0.203851	0.183973
C	0.723812	0.270409	0.185047
C	0.790521	0.203850	0.183858
C	0.924209	0.271178	0.186256
C	0.992275	0.405348	0.191006
C	0.125025	0.471978	0.201168
C	0.189479	0.401120	0.204858
C	0.317006	0.456975	0.222336
C	0.387789	0.401094	0.203108
C	0.524309	0.472330	0.200195
C	0.590683	0.405266	0.190644
C	0.724074	0.470812	0.185901
C	0.790573	0.403722	0.185031
C	0.924135	0.470741	0.186015
C	0.990196	0.603752	0.182723
C	0.123246	0.671093	0.185542
C	0.190612	0.607576	0.198996
C	0.594254	0.608303	0.196827
C	0.725507	0.671389	0.184488
C	0.791149	0.603953	0.182534
C	0.924023	0.670595	0.178830
C	0.990721	0.803883	0.175129
C	0.123972	0.870924	0.175026
C	0.190164	0.804349	0.180470
C	0.323437	0.871052	0.182908

C	0.386392	0.802198	0.194149
C	0.521967	0.866705	0.191968
C	0.593402	0.802612	0.192393
C	0.725252	0.871306	0.181923
C	0.791823	0.804556	0.179578
C	0.924651	0.871071	0.174772
N	0.317493	0.677172	0.208380
N	0.536167	0.677100	0.204623
Fe	0.480335	0.465261	0.336340
Fe	0.398008	0.614635	0.271708

Supplementary references

- 1 G. Rostamikia, S. Maheshwari and M.J. Janik, *Catal. Sci. Technol.*, 2019, **9** 174-181.
- 2 C. Choi, S. Back, N.-Y. Kim, J. Lim, Y.-H. Kim and Y. Jung, *ACS Catal.*, 2018, **8** 7517-7525.
- 3 W. Yang, H. Huang, X. Ding, Z. Ding, C. Wu, I.D. Gates and Z. Gao, *Electrochim. Acta*, 2020, **335**, 135667.
- 4 L. Zhang, X. Ji, X. Ren, Y. Ma, X. Shi, Z. Tian, A.M. Asiri, L. Chen, B. Tang and X. Sun, *Adv. Mater.*, 2018, **30**, 1800191.
- 5 J. Zhao, J. Zhao and Q. Cai, *Phys. Chem. Chem. Phys.*, 2018, **20**, 9248-9255.
- 6 Y. Wang, X. Cui, J. Zhao, G. Jia, L. Gu, Q. Zhang, L. Meng, Z. Shi, L. Zheng, C. Wang, Z. Zhang and W. Zheng, *ACS Catal.*, 2019, **9**, 336-344.
- 7 T. He, A.R. Puente Santiago and A. Du, *J. Catal.*, 2020, **388**, 77-83.